ELSEVIER

Polymer Vol. 37 No. 3, pp. 379–385, 1996

0032-3861/96/$15.00+0.00

polymer papers

High-resolution X-ray photoelectron spectroscopy of crystalline and amorphous poly(ethylene terephthalate): a study of biaxially oriented film, spin cast film and polymer melt

G. Beamson*, D. T. Clark, N. W. Hayes and D. S-L. Law
Research Unit for Surfaces, Transforms and Interfaces, Daresbury Laboratory, Warrington WA4 4AD, UK

and V. Siracusa and A. Recca
Department of Chemistry, University of Catania, 95125 Catania, Italy
(Received 26 April 1995)

High-resolution monochromated X-ray photoelectron spectroscopy (X.p.s.) (core line and valence band) was used to study poly(ethylene terephthalate (PET) as biaxially oriented crystalline film, spin cast amorphous film and amorphous polymer melt. On going from crystalline to amorphous PET the C 1s glycol component shifts $\sim +0.10$ to $+0.14$ eV, relative to the aromatic and carboxyl components. We ascribe this to the change from *trans*- to *gauche*-conformation of the glycol segment. Small differences occur in the valence bands of the crystalline and amorphous samples. Time-dependent studies demonstrate that the melt spectra are not significantly affected by thermal degradation. Under the conditions of the X.p.s. analysis molten PET behaves as an electrical conductor.

(Keywords: X-ray photoelectron spectroscopy; poly(ethylene terephthalate); *trans*-/*gauche*-conformation)

INTRODUCTION

Poly(ethylene terephthalate) (PET) is a technologically important polymer with widespread use in packaging, reprographics and magnetic recording media. It is frequently used as biaxially oriented film, which is produced by stretching in two perpendicular directions above the glass transition temperature ($T_g \sim 80°C$) followed by annealing above 200°C. This treatment induces partial alignment of the molecular chains and crystallization of the material, with a consequent improvement in mechanical, thermal and optical properties[1–3]. Optimization of the film manufacturing process for desired material properties requires the availability of physical methods for the characterization of chain conformation and crystallinity. X-ray diffraction, vibrational spectroscopy, birefringence and density measurements have all been used in the past. Here we describe results from high-resolution X-ray photoelectron spectroscopy (X.p.s.) which form the basis of a method for investigating polymer chain conformation in the uppermost surface layers of PET.

The repeat unit of PET is shown in *Figure 1*. X-ray diffraction demonstrates that in crystalline PET the polymer chains are planar with a *trans*-conformation of oxygen atoms in the glycol segment[4]. Infra-red spectroscopy shows that in amorphous PET the conformation of oxygen atoms in the glycol segment is largely *gauche*[5,6] but with up to $\sim 15\%$ of the *trans*-isomer[7]. Fundamental vibrations associated with the glycol segment occur at different frequencies in the *trans*- and *gauche*-conformations[5,6,8] and measurement of infra-red band intensities may be related to density and the degree of crystallinity[7,9,10]. The technique can be applied to the bulk polymer and, in the form of attenuated total reflectance infra-red (a.t.r. i.r.) spectroscopy, to the near surface region. A.t.r. i.r. spectroscopy typically has a sampling depth $> 0.5\,\mu$m.

The chemical composition of the uppermost surface region (i.e. ~ 5 nm) of PET film is critical to many of its applications and can be monitored routinely by X.p.s. The polymer chain conformation within the X.p.s. sampling depth may also affect surface properties but its determination is less straightforward. *Ab initio* calculations[11] have predicted 'internal' C 1s binding energy shifts of ~ 0.1 eV for polymeric molecules depending on the relative orientation of functional groups, but until now the experimental observation of such shifts has not been reported. A series of papers have predicted small variations in the X.p.s. valence band with polymer conformation[12,13] and have compared theory with experiment[14,15]. In several cases a conclusive

* To whom correspondence should be addressed

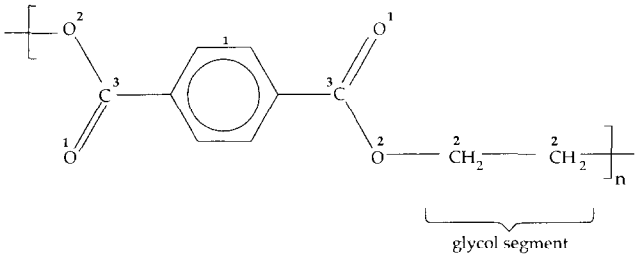

Figure 1 PET repeat unit; indices on C and O atoms correspond to C 1s and O 1s spectral components

dependence of the valence band on polymer chain conformation has been demonstrated[16,17].

Boulanger *et al.*[10] reported core and valence band spectra for crystalline (biaxially oriented film) and amorphous (powder) PET samples, and compared experimental valence bands with *ab initio* calculations for model molecules of PET in the *trans-* and *gauche-*glycol conformations. They suggested that small differences observed in the valence bands of crystalline and amorphous PET are of conformational origin. They also reported a slight increase in linewidth of the C 1s and O 1s components of amorphous PET relative to crystalline material. This could be a conformational effect but is more likely to result from worse differential charging in the amorphous powder sample than in the crystalline film. Limited spectral resolution prevented a definite conclusion to be reached on this point.

In this work we report core and valence band spectra of PET in the form of biaxially oriented crystalline film, spin cast amorphous film and amorphous polymer melt. Our high-resolution spectra demonstrate an unambiguous shift of the C 1s glycol component relative to the aromatic and carboxyl components (corresponding to carbon atoms 2, 1 and 3 respectively in *Figure 1*) upon going from crystalline film to both spin cast film and polymer melt. Small but definite changes are also observed in the valence band spectrum. Time-dependent studies carried out in the analysis chamber of the X-ray photoelectron spectrometer demonstrate that thermal degradation does not significantly affect the melt spectra. We also show that under the conditions of the X.p.s. analysis molten PET behaves, rather surprisingly, as an electrical conductor.

EXPERIMENTAL

The PET samples were analysed by X.p.s. using a Scienta ESCA300 spectrometer. This combines a high-power rotating anode and a monochromatized AlKα X-ray source ($h\nu = 1486.6$ eV) with high-transmission electron optics and a multichannel detector[18,19]. Efficient pumping by liquid-nitrogen-trapped diffusion pumps on the sample analysis chamber, electrostatic lens column and hemispherical analyser/detector chamber allows analysis of highly outgassing samples such as polymer melts. Charge compensation for insulating samples is achieved with a low-energy-electron flood gun. The adjustment of flood gun settings for optimum charge compensation and examples of the resulting high-resolution polymer spectra which can be obtained with an ESCA300 spectrometer have been described previously[20].

Survey, core line and valence band spectra were recorded for each sample at an X-ray source power of 2.8 kW. Survey spectra were acquired at 300 eV pass energy and 1.9 mm slitwidth, core lines at 150 eV pass energy, 0.5 mm slitwidth, and valence bands at 150 eV pass energy, 1.9 mm slitwidth. Under these conditions the instrument resolution is 1.0, 0.32 and 0.55 eV, respectively[21]. For the core lines and valence band a step interval of 0.05 eV was used. The core line and valence band spectra were run on different pieces of the same sample to minimize X-ray and thermal induced degradation, and a short C 1s spectrum was recorded with the valence band to permit binding energy referencing of the two sets of data. Typical acquisition times were $\sim$ 40 min for a set of survey, C 1s and O 1s regions, and $\sim$ 100 min for a survey, C 1s and valence band set.

The following PET samples were studied:

(i) Biaxially oriented film; 125 μm thick (ICI Melinex 'O' grade, as received). A piece of film was cut to fit on a 10 mm diameter stainless steel sample stub and retained with a stainless steel ring (8 mm i.d.) clamped to the stub. The film was analysed at ambient temperature. The survey spectrum showed only C, O and a very small Fe 2p signal from the stainless steel ring.

(ii) Material as in (i) dissolved in hexafluoroisopropanol (Aldrich) to give an $\sim$ 3 wt% solution, and spin cast on to a 13 mm diameter glass microscope cover slip, previously cleaned by wiping with tissue and isopropanol. The cover slip was mounted on a stainless steel stub with double sided tape and analysed at ambient temperature. The survey spectrum showed no contribution from the substrate but a small amount of solvent retained in the spin cast film gave rise to an F 1s signal ($\sim$ 0.8 at%). The corresponding CF_3 signal made only a small contribution to the C 1s spectrum.

(iii) Material as in (i) in the molten state. To achieve this a piece of film was cut to fit on a 10 mm diameter molybdenum stub with an internal resistive heater coil (Vacuum Generators). The film was retained with a stainless steel ring clamped to the stub as in (i). When positioned on the sample manipulator, inside the analysis chamber of the ESCA300 spectrometer, a current could be passed through the heater coil. The arrangement was such that one end of the coil contacted an earthed strip on the manipulator and the other end the stub body. The latter was connected via the manipulator to one side of a floating d.c. power supply, with the other side being earthed. The heater current was slowly increased until the polymer film was seen to melt. A binocular microscope on the analysis chamber directed at the sample, was useful in this respect. Care was required as too rapid heating could result in foaming and serious outgassing of the molten polymer. There was no thermocouple on the manipulator/sample stub and hence the exact sample temperature was unknown, except for it being above the melting point of PET[22], at 265°C. Melting typically occurred at power supply settings of 2.5–3.0 V and 1.5–1.6 A, and caused the pressure in the analysis chamber to rise from $\sim 1 \times 10^{-8}$ mbar to between 5×10^{-8} and 1×10^{-7} mbar. The survey spectrum of the melt

showed only C, O and a very small Fe 2p signal from the stainless steel clamping ring.

For the biaxially oriented film and spin cast PET samples charge compensation using a low-energy-electron flood gun was required. The optimum charge compensation, and hence spectral resolution, was obtained with the sample surface perpendicular to the flood gun beam, resulting in an electron take-off-angle of 45° relative to the sample surface. With typical flood gun settings the first component of the PET C 1s spectrum came at a measured binding energy of ~ 282 eV. Change of sample stub bias voltage over the range +3 to −3 V caused no change of the measured C 1s binding energy. For the molten polymer film external charge compensation was found to be unnecessary, with an entirely satisfactory spectrum being obtained with the flood gun switched off. Hence under the conditions of the X.p.s. analysis molten PET appears to behave as an electrical conductor. This was confirmed by reversing the polarity of the voltage applied across the heater stub and noting a shift in measured binding energy of the C 1s envelope. *Figure 2* shows the corresponding C 1s spectra without any correction to the binding energy scale. The separation of the C 1s envelopes is ~ 4.9 eV, whereas the applied bias change was 5.8 V. The difference is probably due to resistance in the electrical pathway between the power supply and heater stub. Similar electrical conductivity was observed in experiments with other molten polymers and with liquid polymers at ambient temperature. This will be the subject of a future publication[23].

DEGRADATION STUDIES

Molten PET is subject to both thermal and X-ray induced degradation during X.p.s. analysis. This was investigated by recording sets of C 1s and O 1s spectra sequentially over 5–10 h in the following experiments:

(i) Biaxially oriented PET film at ambient temperature was irradiated with monochromatic AlKα radiation at an X-ray source setting of 2.8 kW. The film was also bombarded by low-energy electrons from the flood gun.
(ii) As in (i) but the sample was heated, but not melted, by passing a current of 1 A through the heater stub.
(iii) As in (i) but the sample was heated to above its melting point by passing a current of 1.5 A through the heater stub.

In addition to monitoring the degradation by X.p.s., a quadrupole mass spectrometer on the ESCA300 analysis chamber was used to detect gaseous products.

Experiment (i) showed a decrease in the O/C ratio with time (~ 0.8% h^{-1}) and in the C 1s glycol and carboxyl component intensities relative to the aromatic component. The glycol and carboxyl components decreased at similar rates. The main gaseous degradation products were CO and CO_2. Experiment (ii) gave a similar rate of change of the O/C ratio but the C 1s glycol component decreased faster than the carboxyl component. The main gaseous products were still CO and CO_2 at approximately the same levels as in (i). Experiment (iii) showed a faster decrease of the O/C ratio (approximately twice as fast as in (i) or (ii)) and a higher level of CO, CO_2 and other gaseous products. The glycol component still decreased faster than the carboxyl component. Hence, although melting brings about an increase in degradation rate, within the time required to melt the sample and record a set of survey, C 1s and O 1s spectra (~ 60 min) the overall level of degradation is small (~ 1.5% decrease in the O/C ratio). Even during the longer time required to melt the sample and record survey, C 1s and valence

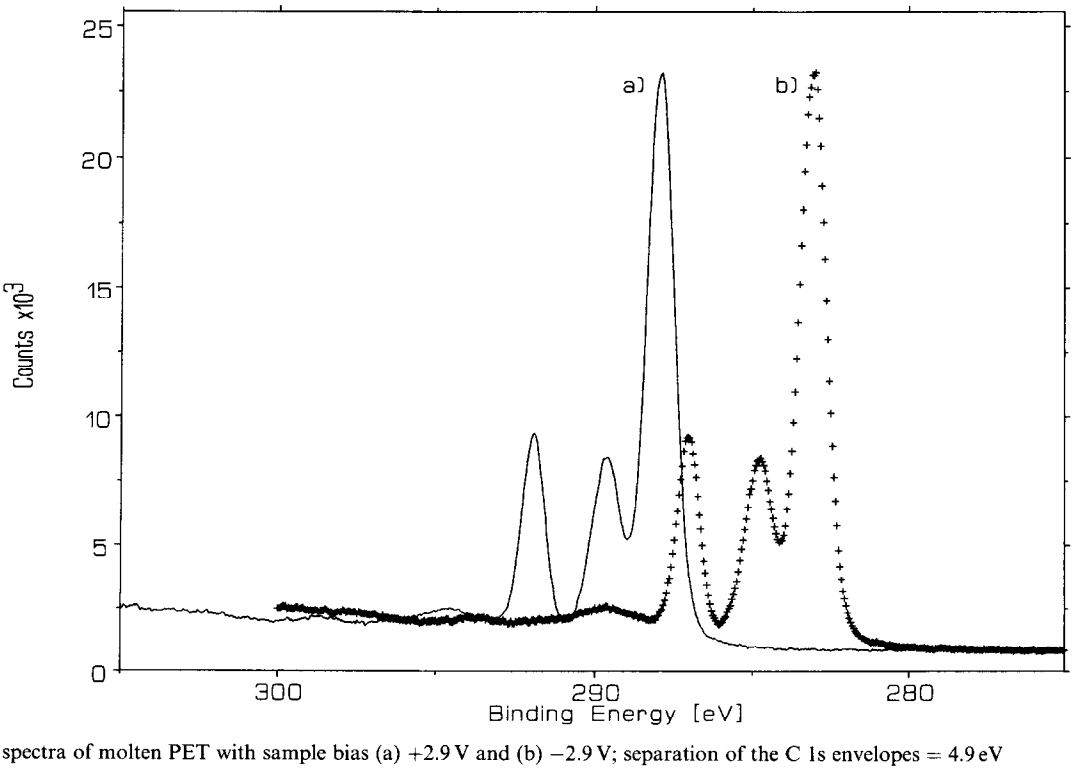

Figure 2 C 1s spectra of molten PET with sample bias (a) +2.9 V and (b) −2.9 V; separation of the C 1s envelopes = 4.9 eV

band spectra (~ 120 min) the decrease in the O/C ratio is still only ~ 3%.

A previous X.p.s. study of thermal degradation in PET[24] showed broadly similar results to those described above, i.e. a decrease in the O/C ratio and in the C 1s glycol and carboxyl components relative to the aromatic component upon heating.

DISCUSSION

Figure 3 shows C 1s and O 1s spectra of the three forms of PET studied and *Figure 4* the corresponding valence band spectra. These spectra are shifted so that the first curve-fit component of the C 1s envelope comes at a binding energy of 284.70 eV. Quantification and curve-fit data for the core line spectra are shown in *Table 1*.

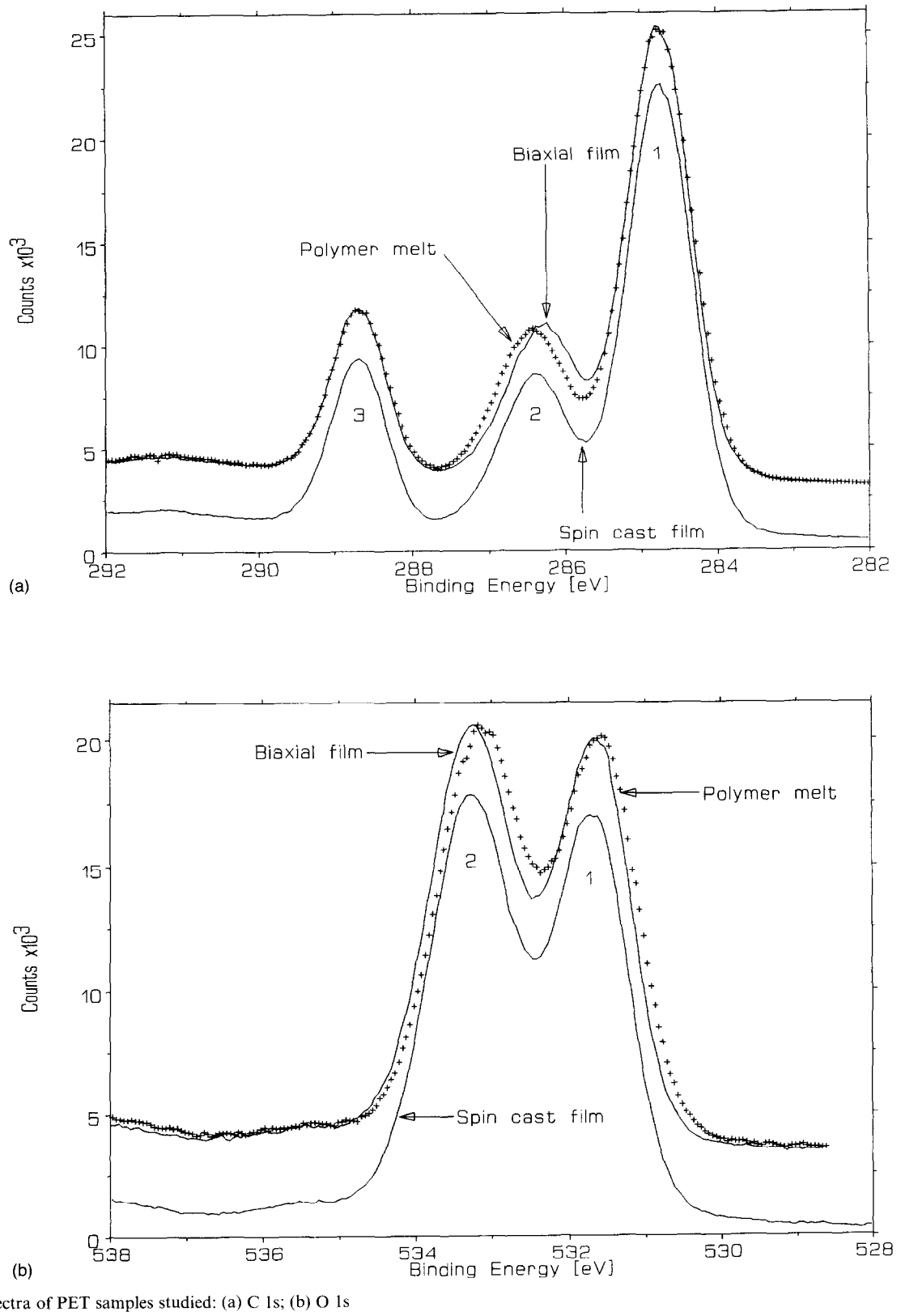

Figure 3 Spectra of PET samples studied: (a) C 1s; (b) O 1s

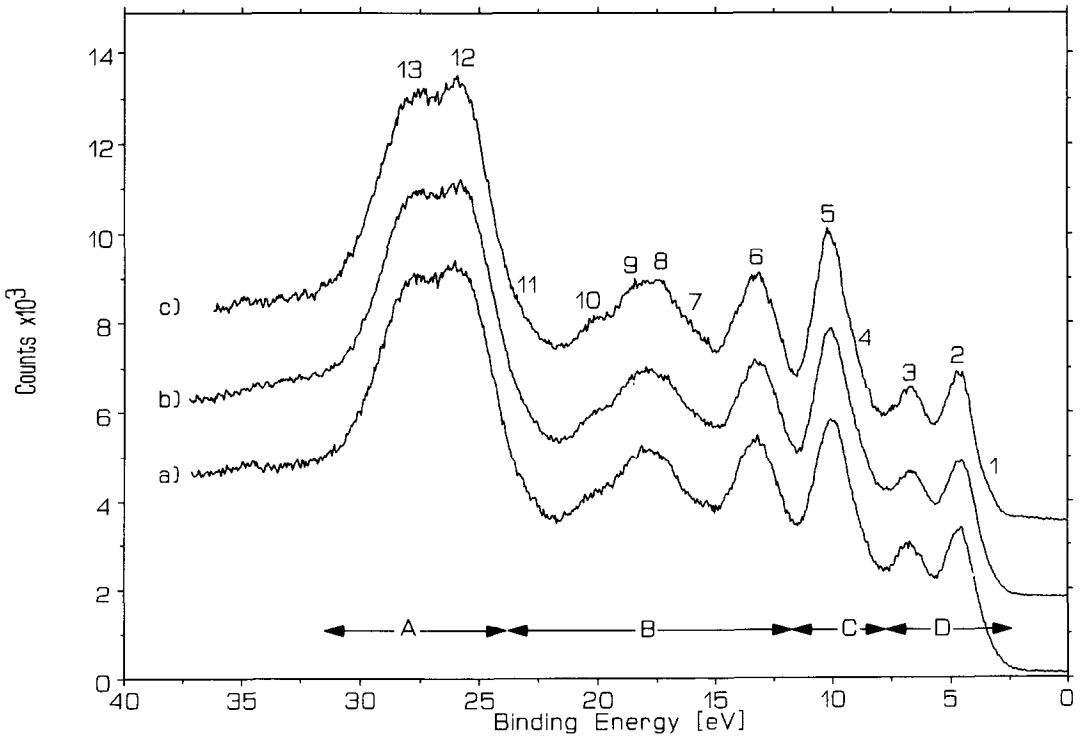

Figure 4 Valence band spectra of PET samples studied: (a) biaxially oriented film; (b) spin cast film; (c) polymer melt

Table 1 Quantification and curve-fit data for PET samples studied[a]

	Quantification (at%)		C 1s Binding energy (eV)			C 1s FWHM (eV)			O 1s Binding energy (eV)		O 1s FWHM (eV)	
Sample	C	O	1	2	3	1	2	3	1	2	1	2
Biaxially oriented film	71.8	28.2	284.70	286.28	288.64	0.98	1.04	0.85	531.61	533.21	1.15	1.33
Spin cast film	71.7	28.3	284.70	286.38	288.65	1.01	1.06	0.87	531.66	533.23	1.16	1.33
Polymer melt	72.2	27.8	284.70	286.42	288.64	1.02	1.03	0.87	531.54	533.11	1.19	1.34
Theory	71.4	28.6	–	–	–	–	–	–	–	–	–	–

[a] FWHM = full width at half maximum

Quantification was achieved with a straight line baseline across the C 1s and O 1s envelopes and using sensitivity factors previously measured on PET film assuming a C/O ratio of 10/4. Curve-fitting was carried out by using the Scienta ESCA300 software[20]. Care was taken during curve-fitting to ensure consistency of shape (Gauss/Lorentzian ratio and asymmetry) and relative area of the core line components for the different PET samples.

Of particular note in the curve-fit data is the increase in binding energy of the C 1s glycol component relative to the aromatic and carboxyl components (components 2, 1 and 3 respectively in *Table 1*) on going from biaxially oriented film to spin cast film and polymer melt. For spin cast film the shift is ~ 0.10 eV and for polymer melt it is ~ 0.14 eV. The shifts are easily seen in the raw data in *Figure 3a* as a deepening of the valley between components 1 and 2. It is clear from X-ray diffraction[4] and infra-red data[5–7] that the conformation of the glycol segment of PET changes from *trans* to largely *gauche* in going from crystalline to amorphous material and we ascribe the observed C 1s glycol shift to the same effect. This is supported by *ab initio* calculations[11] which suggest that conformational effects may cause 'internal' C 1s binding energy shifts of ~ 0.1 eV in polymers, although such calculations have not yet been carried out specifically for PET.

The melt is expected to contain a high fraction of the *gauche*-isomer, indeed infra-red measurements on bulk polymer[7] give a figure of $\sim 85\%$ *gauche*, $\sim 15\%$ *trans* (all in the amorphous phase) for melt quenched PET. The spin cast PET film may contain a higher fraction of *trans*-isomer, thus giving a lower overall shift of the C 1s glycol component. The biaxially oriented film is known to have a bulk crystallinity[22] of $\sim 56\%$, hence the *trans*-content will be at least this and there will be additional *trans*-material in the amorphous phase of the sample. Grazing incidence X-ray diffraction[25] shows that the uppermost 9 nm of aromatic polyimide film is markedly more ordered than the bulk and the same may apply to other polymers such as PET. Hence it is difficult to estimate the actual fraction of *trans*-material at the surface of biaxially oriented PET film except that it is considerably greater than in spin cast film or in the melt. Nevertheless, the trend in binding energy of the C 1s

glycol component is clear and may be used to provide an indication of the amount of *trans*-isomer at the surface.

The data in *Table 1* show no significant difference in separation of the O 1s components for the three PET samples studied, although there is a variation in position of the O 1s envelope relative to C 1s. The O 1s envelope of the polymer melt is ~ 0.1 eV lower in binding energy than that of either the biaxially oriented or spin cast films. As the melt is electrically conducting this could represent a slight differential charging effect across the binding energy scale, present for the two solid insulating samples but absent for the melt. It is interesting to note that the full width at half maximum (FWHM) of the curve-fit components are nominally the same for the conducting melt as for the two insulators, suggesting that lateral and depthwise differential charging does not significantly affect the spectra of the insulators. The reason for the electrical conductivity of molten PET is not yet clear but could arise from the diffusion of small ions created by photoionization through the liquid[23].

The valence band spectrum of PET, shown in *Figure 4*, suggests a total of 13 spectral components. These may be divided into 4 spectral regions[10,26] representing photoionization from molecular orbitals in which the dominant atomic contributions are as follows: region A (24–31 eV binding energy range, components 12 and 13), O 2s; region B (12–24 eV binding energy range, components 6–11), C 2s and O 2s; region C (8–12 eV binding energy range, components 4 and 5), C 2p, O 2p and H 1s; region D (2.5–8 eV binding energy range, components 1–3), C 2p and O 2p. The valence band shows several small changes on going from biaxially oriented film to spin cast film and polymer melt. In particular, component 5 increases in height relative to 6 and the two peaks move closer together. Peak-fitting suggests that in biaxially oriented film the separation is ~ 3.25 eV, whereas in spin cast film and polymer melt it is ~ 3.10 eV. Components 8 and 10 are also more prominent in the two amorphous samples. The increased height of component 5 in amorphous PET is apparent in the data of Boulanger *et al.*[10], as are the changes in the region spanned by components 7–10. Calculations[10,26] show that component 5 represents photoionization from several molecular orbitals, including those involved in the C–C, C–O and C–H bonds of the glycol segment. The binding energies of these orbitals may shift on going from *trans*- to *gauche*-glycol conformation giving, fortuitously, an increased height for component 5 in amorphous PET.

The differences in the valence band between crystalline and amorphous PET are subtle and lack the clarity of the C 1s glycol shift. In addition, the X.p.s. valence band is ~ 30 times weaker than the C 1s line. Hence in terms of monitoring polymer chain conformation at the surface of PET, measurement of the C 1s glycol shift seems to be the method of choice.

CONCLUSION

We have used high-resolution X.p.s. to study PET in the form of biaxially oriented crystalline film, spin cast amorphous film and amorphous polymer melt. Time-dependent studies show that within the time required to record the melt data, thermal degradation has only a small effect on the appearance of the spectra.

It is known from X-ray diffraction and infra-red data that the crystalline-to-amorphous transition in PET involves a change in conformation of the glycol segment from *trans* to largely *gauche*. Our X.p.s. data demonstrate an unambiguous shift of the C 1s glycol component, relative to the aromatic and carboxyl components, on going from biaxially oriented crystalline film to amorphous PET. For spin cast PET the shift is +0.10 eV and for molten PET it is +0.14 eV. *Ab initio* calculations[11] suggest conformational-dependent 'internal' C 1s shifts of this order, and we ascribe the C 1s glycol shift to the change in conformation of the glycol segment from *trans* to *gauche*. Calculations specifically on PET are required to fully confirm this. The C 1s glycol shift forms the basis of a method for investigating polymer chain conformation in the uppermost surface layers of PET and is of potential technological importance.

Our data also demonstrate small changes in the valence band on going from crystalline to amorphous PET. The most obvious of these is the increased height in amorphous PET of the component at ~ 10 eV binding energy, which includes photoionization from molecular orbitals associated with the glycol segment.

Finally, we note that under the conditions of the X.p.s. analysis molten PET behaves as an electrical conductor. Other molten polymers and liquid polymers at room temperature show similar behaviour. Hence the phenomenon appears to be general and may be due to diffusion through the liquid of small ions created by photoionization.

ACKNOWLEDGEMENT

We acknowledge the UK Engineering and Physical Sciences Research Council for financial support of the RUSTI core programme. Dr D. Briggs at ICI Wilton is thanked for provision of PET samples and helpful discussion.

REFERENCES

1 McCrum, N. G., Buckley, C. P. and Bucknall, C. B. 'Principles of Polymer Engineering', Oxford University Press, Oxford, 1988
2 ICI Films information note No. 16, Middlesbrough, 1995
3 Gohil, R. M. *J. Appl. Polym. Sci.* 1994, **52**, 925
4 Daubeny, R. de P., Bunn, C. W. and Brown, C. J. *Proc. R. Soc. London, Ser. A* 1954, **286**, 531
5 Miyake, A. *J. Polym. Sci.* 1959, **38**, 479
6 Miyake, A. *J. Polym. Sci.* 1959, **38**, 497
7 Lin, S. B. and Koenig, J. L. *J. Polym. Sci., Polym. Phys. Edn* 1982, **20**, 2277
8 D'Esposito, L. and Koenig, J. L. *J. Polym. Sci., Polym. Phys. Edn* 1976, **14**, 1731
9 Yazdanian, M., Ward, I. M. and Brody, H. *Polymer* 1985, **26**, 1779
10 Boulanger, P., Pireaux, J. J., Verbist, J. J. and Delhalle, J. *J. Electron Spectrosc. Relat. Phenom.* 1993, **63**, 53
11 Meier, R. J. and Pijpers, P. J. *Theor. Chim. Acta* 1989, **75**, 261
12 Boulanger, P., Lazzaroni, R., Verbist, J. and Delhalle, J. *Chem. Phys. Lett.* 1986, **129**, 275
13 Hennico, G., Delhalle, J., Boiziau, C. and Lecayon, G. *J. Chem. Soc. Faraday Trans.* 1990, **86**, 1025
14 Orti, E., Bredas, J. L., Pireaux, J. J. and Ishihara, N. *J. Electron Spectrosc. Relat. Phenom.* 1990, **52**, 551
15 Boulanger, P., Riga, J., Verbist, J. J. and Delhalle, J. 'Polymer–Solid Interfaces' (Eds J. J. Pireaux, P. Bertrand and J. L Bredas), IOP Publishing, Bristol, 1992, p. 315
16 Boulanger, P., Riga, R., Verbist, J. J. and Delhalle, J. *Macromolecules* 1989, **22**, 173

17 Riga, J., Delhalle, J., Deleuze, M., Pireaux, J. J. and Verbist, J. J. *Surf. Interface Anal.* 1994, **22**, 507
18 Beamson, G., Briggs, D., Davies, S. F., Fletcher, I. W., Clark, D. T., Howard, J., Gelius, U., Wannberg, B. and Balzer, P. *Surf. Interface Anal.* 1990, **15**, 541
19 Gelius, U., Wannberg, B., Baltzer, P., Fellner-Feldegg, H., Carlsson, G., Johansson, C-G., Larsson, J., Munger, P. and Vegerfors, G. *J. Electron Spectrosc. Relat. Phenom.* 1990, **52**, 747
20 Beamson, G. and Briggs, D. 'High Resolution XPS of Organic Polymers. The Scienta ESCA300 Database', Wiley, Chichester, 1992
21 ESCA300 Instrument Manual, Scienta Instruments AB, Uppsala, 1988
22 ICI Melinex Technical Data Sheet MX TD306, 4th Edn, ICI, Middlesbrough, 1985
23 Beamson, G., unpublished results
24 Clark, D. T. and Abu-Shbak, M. M. *Polym. Degrad. Stab.* 1984, **9**, 225
25 Factor, B. J., Russel, T. P. and Toney, M. F. *Phys. Rev. Lett.* 1991, **66**, 1181
26 Chtaib, M., Ghijsen, J., Pireaux, J. J., Caudano, R., Johnson, R. L., Orti, E. and Bredas, J. L. *Phys. Rev. B* 1991, **44**, 10815